

Chapter

Charge Carriers for Next-Generation Redox Flow Batteries

Catherine L. Peake, Graham N. Newton and Darren A. Walsh

Abstract

Increasing the volumetric energy density of redox flow batteries beyond that of the archetypal all-vanadium system requires the development of highly soluble charge carriers that can store multiple electrons per charge cycle. In this review article we will describe the design and performance of a range of new charge carriers for flow batteries, with an emphasis on those with multi-electron redox properties. These include fullerene derivatives, multifunctional organic systems, metal coordination complexes, and polyoxometalates. Our discussion will include an evaluation of the fundamental physical and electrochemical properties of the charge carriers and their impact on battery performance and energy density.

Keywords: multi-electron charge carriers, flow battery, electrolyte, next-generation batteries, energy density

1. Introduction

High-capacity, cost effective and durable electrochemical energy storage technologies are necessary to satisfy the growing uptake of intermittent renewable sources and maintain stable electrical-grid systems [1]. In this regard, redox flow batteries (RFBs) are ideally suited and have attracted considerable attention. RFBs differ from conventional batteries in that redox-active molecules, termed charge carriers, are dissolved into electrolyte and are stored in reservoirs external to the electrochemical cell. The charge carrier-containing electrolyte is pumped through electrodes in the electrochemical cell to charge/discharge the battery. Upon charge, energy is stored as the positive electrolyte (also termed catholyte or posolyte) is oxidised and the negative electrolyte (also termed anolyte or negolyte) is simultaneously reduced. Upon discharge, energy is released as the redox reactions are reversed. The electrolytes are separated in the cell by a membrane or separator, which allows transfer of charge-balancing counterions but prevents crossover of charge carriers to the opposite half-cell, thus preventing self-discharge. **Figure 1** shows a schematic of a generic RFB under discharge conditions.

The distinctive design of RFBs allows decoupling of energy and power, and therefore facile scale-up to high capacities [3]. Capacity can be enhanced by simply

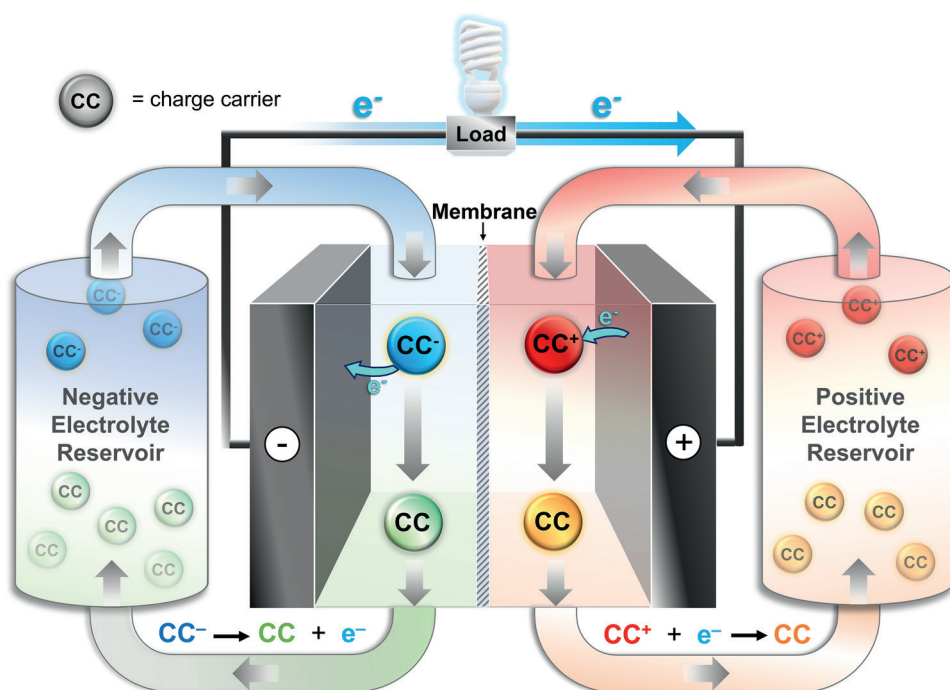


Figure 1. Schematic of a generic RFB under discharge conditions. Electrolytes are stored in reservoirs and are pumped through the electrochemical cell to charge and discharge the battery. Upon discharge the charge carriers in the positive electrolyte are reduced while those in the negative electrolyte are oxidised. Polarity is reversed to allow the opposite redox reactions to occur upon charge. Reproduced from [2] with permission from the Royal Society of Chemistry.

increasing the volume of electrolyte in the reservoirs, without the need to modify the electrochemical cell, while power is determined by the cell design (e.g. electrode surface area etc). Furthermore, in contrast to conventional batteries such as the lithium-ion battery (LIB), RFBs avoid the intercalation and deintercalation of redox-active molecules between the electrolyte and solid electrode material. Instead, redox reactions occur via solution phase charge carriers at the electrode surface. This underpins the long operational lifetimes of RFBs (15–20 years), making them particularly suited to grid-scale energy storage.

Historically, RFBs have relied on charge carriers based on metals such as iron, chromium, zinc, or cerium, dissolved in aqueous electrolyte [4]. The earliest investigations were conducted by the National Aeronautics and Space Administration (NASA) in the 1970s. Their most notable development was the iron-chromium RFB which used $\text{Fe}^{2+}/\text{Fe}^{3+}$ and $\text{Cr}^{2+}/\text{Cr}^{3+}$ in the positive and negative electrolytes respectively [5]. Scale-up and commercialisation of the system were hindered by several technical challenges including the slow electron transfer kinetics of $\text{Cr}^{2+}/\text{Cr}^{3+}$ [4]. Today, the most commercially advanced RFB system is the symmetric, all-vanadium RFB developed by Skyllas-Kazacos and co-workers in the late 1980s [6, 7]. The charge carriers in the system are $\text{VO}_2^+/\text{VO}^{2+}$ ($\text{V}^{5+}/\text{V}^{4+}$) in the positive electrolyte and $\text{V}^{2+}/\text{V}^{3+}$ in the negative electrolyte. Vanitec lists 33 companies commercialising all-vanadium RFBs [8] and several plants have been installed globally. The largest electrochemical energy storage plant in the world is forecast to be a 200 MW/800 MWh all-vanadium RFB and is under construction by Rong Power of China [3].

Despite their advantages for grid-scale energy storage, commercial uptake of the all-vanadium RFB is dwarfed by that of LIBs due to several drawbacks. Firstly, the cost of the all-vanadium RFB was estimated at \$500 kWh⁻¹ in 2014 [9], which far exceeds the target of \$100 kWh⁻¹ set by the US Department of Energy [10], and the ever decreasing cost of LIBs estimated at \$156 kWh⁻¹ in 2020 [11]. Secondly, the energy density of the all-vanadium RFB is an order of magnitude lower than LIBs [2]. The limited solubility of vanadium sulphate in aqueous solution and the cell voltage of approximately 1.3 V (dictated by the difference in redox potential between the reaction at the positive and negative electrode), limits the energy density to 25–35 Wh L⁻¹ [12]. While lower energy densities are generally more tolerable for stationary rather than portable applications, there is a demand to enhance RFB energy density to cut cost, reduce space requirements and access new markets.

Energy density is a measure of the energy output per unit volume of total electrolyte and is defined in Eq. (1);

$$\text{Energy density} = \frac{n V_{\text{cell}} C F}{2} \quad (1)$$

where n is the number of electrons transferred per molecule in the charge/discharge redox reaction, V_{cell} is the average cell voltage, C is the concentration of charge carrier in the electrolyte, and F is the Faraday constant. The division by two accounts for the necessity for two volumes of electrolyte for a given energy output (positive and negative electrolyte). Furthermore, fast electron transfer kinetics and high stability of the charge carrier are crucial to achieve high power density and long cycle and calendar life. In this regard, charge carriers underpin the energy density and performance of RFBs, and strongly influences the overall cost and sustainability too.

As indicated in Eq. (1), an effective strategy to enhance the energy density of RFBs is to increase the value of n . This is achieved by designing carriers capable of being reversibly reduced/oxidised by multiple electrons per molecule. So called multi-electron charge carriers have a second advantage in that they can often be applied in symmetric systems, where the same charge carrier in different oxidation states is used in the positive and negative electrolyte. In the event of charge carrier transport through the membrane to the opposite half-cell (termed crossover), capacity fade is easily regenerated in symmetric systems as demonstrated in the all-vanadium RFB [12]. Conversely, asymmetric systems, which use a different charge carrier in the positive and negative electrolyte, often suffer from permanent capacity losses.

In the last two decades, research has shifted from metal-based charge carriers in aqueous solution to a new generation of charge carriers with tuneable physical and electrochemical properties to include inorganic, organic, and hybrid materials. In an effort to increase V_{cell} , there has been a growing interest in the development of non-aqueous electrolytes with wide windows of electrochemical stability [13]. Research has focused on designing charge carriers with high solubility in the chosen solvent, and rich electrochemistry at extreme potentials to maximise C , n and V_{cell} respectively. While each of these properties are paramount to enhance energy density, here, we focus on recent advances in the development of multi-electron charge carriers.

Figure 2 shows the components of a typical laboratory-scale RFB used for assessing the performance of charge carriers. Electrolyte is circulated via tubing between the reservoirs and electrochemical cell (typically powered by a peristaltic pump). Within the electrochemical cell, electrolyte is flowed through high surface area

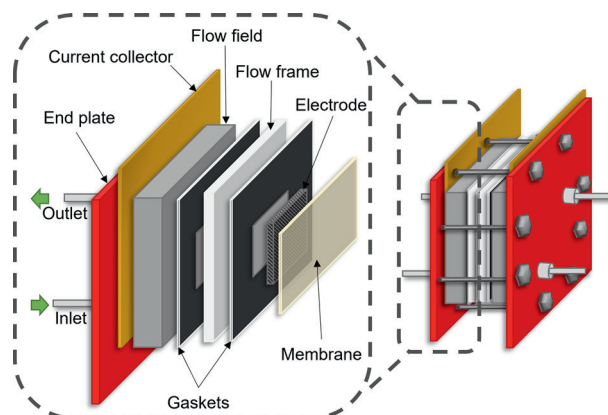


Figure 2.

Schematic of a typical laboratory-scale RFB used for assessing the performance of charge carriers. Battery components include the membrane/separator, electrodes, gaskets, flow frames, flow fields, current collectors, end plates, tubing, pump*, and electrolyte reservoirs*. * not pictured in schematic.*

electrodes where the redox reactions occur upon charge/discharge. The electrodes are typically composed of a carbon-based material such as graphite felt and are electrically connected to the current collectors and external circuit. The flow field (available in several configurations) ensures consistent flow of electrolyte to the porous electrode while minimising pressure drop across the cell.

The membrane/separator divides the two half-cells and should be highly conductive, selective, and stable towards the electrolyte. High ionic conductivity is key to reduce ohmic resistance and thereby enable high power densities to be achieved. Membranes should allow transport of inert salts while preventing crossover of charge carriers, which can lead to capacity fade and reduced coulombic efficiency. Membranes/separators can be broadly classified as porous separators (separating based on size) and ion exchange membranes (separating based on charge). Identifying the most appropriate membrane/separator for novel RFB systems, where the chemistry is not fully understood, can be challenging. This is particularly true in the case of non-aqueous RFBs because very few commercially available membrane/separators have adequate performance in organic solvents [14]. Membranes present a barrier towards commercialisation for many next-generation RFBs since their inadequate performance reduces energy efficiency and they contribute up to 20% of the battery cost [15].

2. Organic charge carriers

There is a growing interest in the development of organic charge carriers as alternatives to metal-centred species, due to their tuneable properties and natural abundance of their elemental building blocks (C, H, N and O). Organic charge carriers investigated to date include nitroxide radicals such as 2,2,6,6-tetramethylpiperidinyloxy (TEMPO), carbonyls such as fluorenone, benzophenone, phthalimides, quinones and anthraquinones, heterocyclic aromatics such as viologens, phenazines and phenothiazine, and cationic radicals such as dialkoxybenzenes and cyclopropenium, to name a few. **Figure 3** showcases a ‘potential map’ of organic charge carriers developed for next-generation RFBs in recent years. We direct the interested reader to consult review articles for further reading on organic charge carriers [13, 16–19].

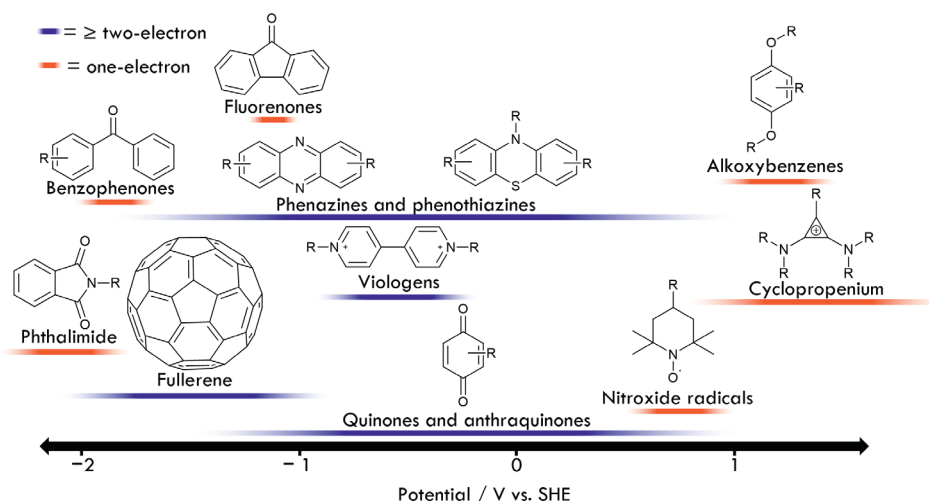


Figure 3. Schematic showing the structure of organic charge carriers investigated for RFBs and the potential region in which they are redox-active. Orange bars indicate species that undergo one-electron redox reactions while those with blue bars are multi-electron charge carriers.

Several organic charge carriers such as viologens, quinones and phenazines, undergo two-electron redox reactions and have been investigated for RFBs. However, the π -conjugated cage structure of fullerene gives it uniquely rich electrochemical properties compared to other organic redox-active molecules. It can be reversibly reduced by up to six electrons at negative redox potentials, making it a desirable charge carrier for the negative electrolyte in RFBs. Without molecular modification, fullerene is nonpolar and unable to partake in hydrogen bonding, meaning its solubility in many solvents is poor [20]. Consequently, fullerene was first investigated as a charge carrier in RFBs as a bifunctional molecule where ferrocene groups (Fc) were covalently grafted to a C_{60} fullerene cage [21]. The functionalisation significantly enhanced the solubility of fullerene in ortho-dichlorobenzene (oDCB) from 0.037 M [22] to 0.12 M for the tetra-adduct of C_{60} Fc. The ferrocene groups served as the redox centre for the positive electrolyte, while the multi-electron redox processes of fullerene were accessed in the negative electrolyte. To balance the redox processes of fullerene, multiple ferrocene moieties were grafted to C_{60} ($x = 1-4$, where x indicates the number of ferrocene groups). The redox processes of the positive and negative electrolyte were separated by approximately 1.3 V and 1.8 V for the first and second reduction of C_{60} respectively. **Figure 4** shows the structure of the fullerene-ferrocene bifunctional charge carriers, termed C_{60} Fc, and the redox reactions occurring in the positive and negative electrolytes upon charge in the RFB.

The performance of C_{60} Fc charge carriers with $x = 2-4$ were investigated by galvanostatic cycling in coin cells. Charge carriers were assessed in symmetric and asymmetric configurations where indene- C_{60} bis-adduct was used as negative electrolyte. The coin cells were successfully cycled for 100 charge-discharge cycles but experienced considerable capacity fade which was attributed to three causes: (1) the low volume of electrolyte (~1 mL) in the coin cell assemblies meant that a significant proportion of capacity fade was attributed to electrolyte soaking into the absorbent glass fibre separator, (2) significant membrane crossover, which was alleviated by using the symmetric system rather than an analogous asymmetric system with indene- C_{60} bis-adduct negative electrolyte, (3) degradation of C_{60} Fc charge carriers,

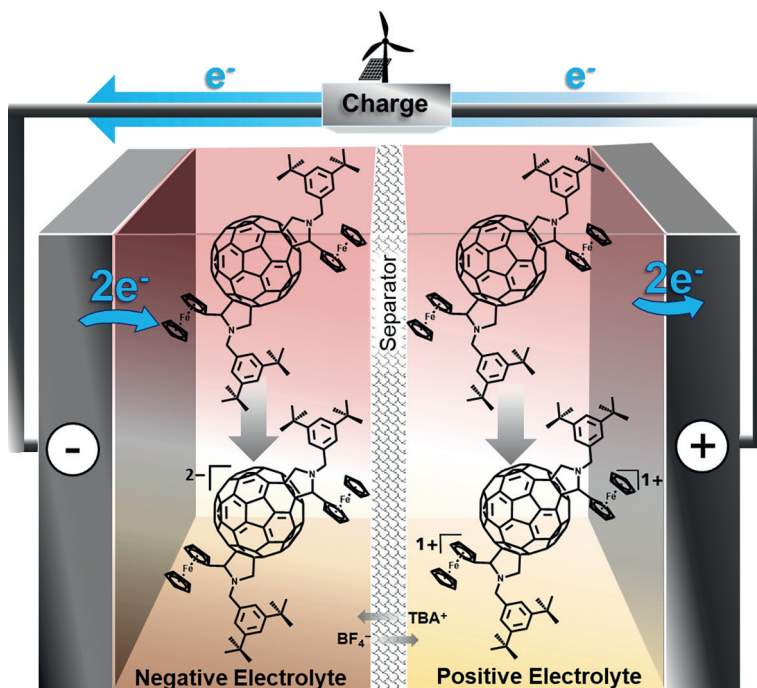


Figure 4. Schematic showing the redox reactions of $C_{60}Fc$ (bis-adduct) in a symmetric non-aqueous RFB. Upon charge, $C_{60}Fc$ in the positive electrolyte undergoes a two-electron oxidation centred at the two ferrocene moieties. Simultaneously, $C_{60}Fc$ in the negative electrolyte is reduced by two electrons at the fullerene core to a dianion. The reverse reactions occur upon discharge.

which was not explored in detail. Considering the rich electrochemistry and plentiful opportunities for functionalisation of fullerene, there is great scope for development of new fullerene-based charge carriers in the future.

The concept of combining two redox-active components into one bifunctional molecule was first demonstrated by Schubert and co-workers, who tethered TEMPO and phenazine moieties to a single molecule [23]. Upon charge, TEMPO was oxidised to an oxoammonium cation in the positive electrolyte while phenazine was simultaneously reduced to a dianion in the negative electrolyte. As shown in **Figure 5**, the bifunctional charge carrier contains two TEMPO groups (red) per phenazine (blue) in order to balance its two-electron redox chemistry. Both redox groups were covalently bonded via a water-soluble triethylene glycol linker (black), yielding a single charge carrier with V_{cell} of 1.2 V when applied in a symmetric RFB. The molecular engineering has a two-fold benefit in that it allows for its application in a symmetric system and enhances the saturation concentration in aqueous electrolyte beyond that of non-functionalised TEMPO and phenazine.

The advantage of symmetric systems in minimising capacity fade upon crossover can also be achieved by using a mixture of the positive and negative charge carriers in each half-cell. To justify the synthetic effort of bifunctional charge carriers, they must show advantageous properties compare to a mixture of the two individual redox-active molecules. In the two examples highlighted above, the bifunctional charge carriers have greater solubility than the individual redox-active groups and therefore a great theoretical energy density is achieved.

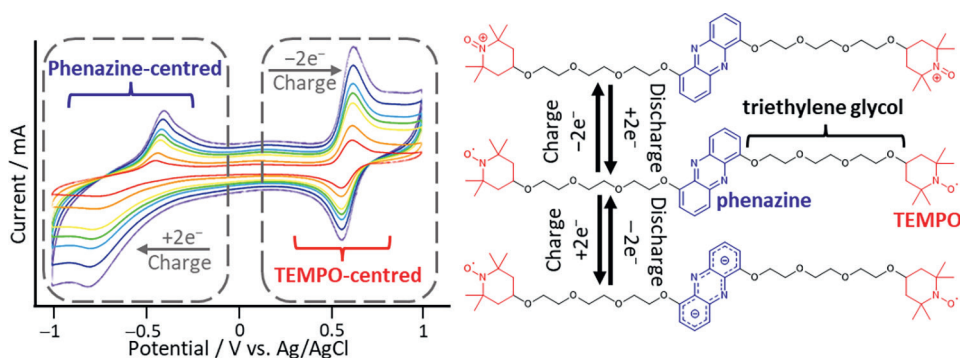


Figure 5. Schematic showing the structure, redox reactions and cyclic voltammogram of a TEMPO-phenazine bifunctional charge carrier. Figure was adapted with permission from [21] copyright © 2016, American Chemical Society.

3. Coordination complex charge carriers

Transition metal coordination complexes are promising candidates for non-aqueous RFBs as they are often stable over multiple oxidation states and their properties are tuneable [24]. The first metal coordination complex to be investigated as charge carrier for non-aqueous RFBs was the ruthenium bipyridine (bpy) complex, $[\text{Ru}(\text{bpy})_3]^{2+}$ [25]. Bpy ligands not only solubilise the metallic cation, they also provide additional redox activity to the molecule. In a symmetric system the $\text{Ru}^{2+}/\text{Ru}^{3+}$ transition was targeted in the positive electrolyte while the bpy-centred reduction was targeted in the negative electrolyte. The redox processes were separated by 2.6 V, allowing for a high V_{cell} , but poor coulombic and voltage efficiencies were observed upon cycling. Within the last decade a range of metal-ligand combinations have been investigated to include nickel, cobalt, iron, vanadium, and chromium metal centres and acetylacetonate, terpyridine and dithiolene ligands to name a few [24]. Ligand design can have a remarkable impact of the charge carrier solubility, stability and redox properties and is therefore a key research focus for optimisation of metal coordination complexes. We direct the interested reader to two recent reviews for a more thorough examination of metal coordination complexes in RFBs [24, 26].

The chromium-centred bpy coordination complex, $[\text{Cr}(\text{bpy})_3]^{3+}$ is of particular note due to its six one-electron reversible redox processes over a 2 V window (see **Figure 6**) [27]. The three most positive redox couples were attributed to the $\text{Cr}^{3+}/\text{Cr}^{2+}$, $\text{Cr}^{2+}/\text{Cr}^{1+}$ and $\text{Cr}^{1+}/\text{Cr}^0$ transitions, while the three most negative redox processes were ascribed to reduction of the three bpy ligands. The authors sought to enhance solubility in acetonitrile through ester-functionalisation of the bpy ligands. The complex functionalised with the most polar and flexible R group (2-(2-methoxyethoxy)ethyl) showed the most promising redox properties and solubility and was selected for battery testing. Galvanostatic cycling in a H-cell showed poor cycling stability when charged by three electrons but relatively stable performance when charged by two. The saturation concentration of both the neutral and 3+ complexes was tested and as anticipated the solubility was dramatically reduced in the neutral form. Despite the promising multi-electron redox properties of $[\text{Cr}(\text{bpy})_3]^{3+}$, the poor solubility of the neutral complex (0.21 M in acetonitrile) and inadequate stability upon cycling, meant that the energy density of the system was limited to 10.2 Wh L^{-1} .

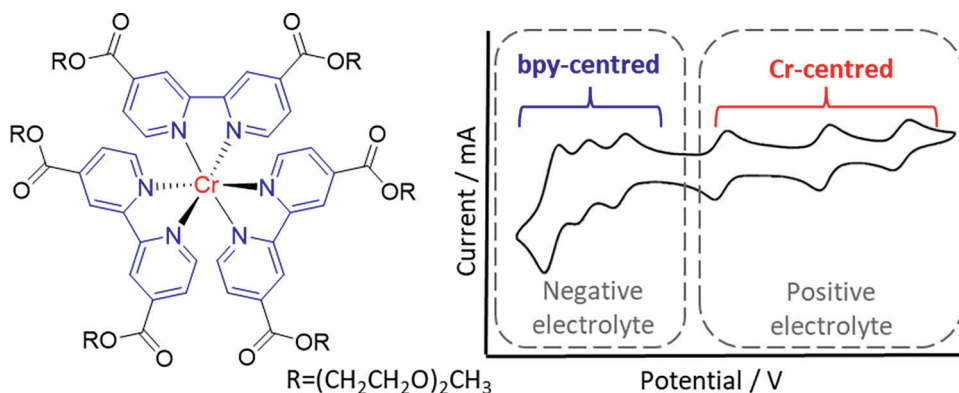


Figure 6.

Structure and cyclic voltammogram of functionalized $[Cr(bpy)_3]^{3+}$ coordination complex investigated for symmetric non-aqueous RFBs. Figure was adapted with permission from [25] copyright © 2015, American Chemical Society.

4. Polyoxyometalate charge carriers

Polyoxometalates (POMs) are a class of discrete metal-oxide nano clusters composed of early transition metals (group 5 and 6) in their highest oxidation states. They can be represented by the general formula $[X_xM_mO_y]^{n-}$ where X is a hetero atom (usually P, Si, Ge, As) and M is a transition metal (typically V^{5+} , Mo^{6+} or W^{6+}). Their vast structural diversity, excellent stability and rich electrochemistry has seen their investigation for many energy conversion and storage technologies [28].

The earliest work on POM-based charge carriers for RFBs was conducted by Anderson and co-workers, who used the tri-vanadium substituted silicotungstate Keggin, $K_6H[SiV_3W_9O_{40}]$ (SiV_3W_9), in a symmetric aqueous system [29]. The POM undergoes a three-electron reduction centred at the vanadium metals and a further two, two-electron reduction processes centred at the tungsten metals. The vanadium-centred redox processes were separated from those of the tungsten by 0.8 V allowing for the application of SiV_3W_9 in a symmetric system. Prior to galvanostatic cycling, the charge carrier was reduced to $[SiV_3W_9O_{40}]^{13-}$ by bulk electrolysis to generate the fully charged negative electrolyte. Galvanostatic cycling in a 5 cm^2 RFB showed coulombic efficiency of $>95\%$ and modest capacity fade of $<2\%$ after 100 cycles (0.02% per cycle). Following 100 cycles, the electrolyte solution was recovered and used in a fresh cell with a new membrane. Full cell performance was restored suggesting that any capacity losses observed were not the result of POM degradation. Given the saturation concentration of SiV_3W_9 in water of 0.45 M, the three-electron redox reaction upon charge/discharge and V_{cell} of approximately 0.8 V, the theoretical volumetric energy density was calculated to be 14.5 Wh L^{-1} . While the energy density is half that of the all-vanadium RFB, this publication pioneered a new class of charge carrier with stable multi-electron redox processes.

Lu and Xiang extended the library of POM-based charge carriers to include the cobalt-centred tungstic acid, $H_6[CoW_{12}O_{40}]$ (CoW_{12}) [30]. Similarly to SiV_3W_9 , the tungsten-centred redox processes of the POM were targeted in the negative electrolyte (two, two-electron reduction processes), while in this case, the one-electron oxidation of the central cobalt atom from $2+$ to $3+$ was targeted in the positive electrolyte. The separation of the cobalt- and tungsten-centred redox processes allowed for

a larger V_{cell} of 1.25 V (0.8 V for SiV_3W_9). However, the positive electrolyte required four equivalents of CoW_{12} to balance the four-electron redox process occurring in the negative electrolyte. The laboratory-scale flow battery achieved coulombic efficiency >98% and good capacity retention over 30 cycles. Given the saturation concentration of CoW_{12} in water of 0.8 M, the theoretical volumetric energy density was calculated to be 16.8 Wh L^{-1} (accounting for necessary balance of POM equivalents in the positive and negative electrolyte).

Stimming and colleagues sought to maximise the rich electrochemistry of POMs by designing an asymmetric RFB with different POM-based charge carriers in the positive and negative electrolyte [31]. They investigated an asymmetric aqueous RFB using $[\text{PV}_{14}\text{O}_{42}]^{9-}$ (PV_{14}) and $[\text{SiW}_{12}\text{O}_{40}]^{4-}$ (SiW_{12}) as charge carriers for the positive and negative electrolyte respectively. PV_{14} is reversibly reduced by seven electrons in a single process at a relatively positive redox potential of 0.60 V vs. standard hydrogen electrode (SHE). The cyclic voltammogram of SiW_{12} has two reversible one-electron reduction processes with redox potentials of 0.01 V and -0.21 V vs. SHE. SiW_{12} can be reduced by a further two-electrons but only the first two one-electron redox couples are accessible without significant hydrogen evolution. Consequently, a flow cell was assembled with two equivalents of SiW_{12} ($n = 2$) to balance the multi-electron redox process of PV_{14} ($n = 4$). Prior to galvanostatic cycling, PV_{14} was reduced by the addition of hydrazine to attain the discharged positive electrolyte. With an average V_{cell} of approximately 0.8 V and limited solubility of PV_{14} (demonstrated at 0.3 M), the theoretical energy density was calculated to be 13 Wh L^{-1} . Successful charge-discharge cycling was demonstrated in a 25 cm^2 flow cell and later upscaled to a 1400 cm^2 system, which remained stable of a 3 month period [32]. This provided a rare example of a next-generation RFB systems being tested at scale for extended periods of time. Capacity fade was attributed to the reoxidation of reduced POMs from trace oxygen which could be avoided with an airtight setup.

A step change in energy density came from the work of Cronin and co-workers where $\text{Li}_6[\text{P}_2\text{W}_{18}\text{O}_{40}]$ (P_2W_{18}) was reversibly reduced by 18 electrons in aqueous acidic conditions [33]. The authors found that the electrochemical properties of P_2W_{18} was highly dependent on pH and concentration and that reversible reduction by 18 electrons was only achievable at concentrations >100 mM under acidic conditions. Paired with HBr/Br_2 positive electrolyte, the asymmetric RFB demonstrated a V_{cell} of 1.25 V equating to a practical energy density of 225 Wh L^{-1} . Extrapolated to the saturation concentration of P_2W_{18} in water of 1.9 M, and assuming equivalent concentrations are achievable in the presence of supporting electrolyte, the authors calculate a theoretical energy density of $>1000 \text{ Wh L}^{-1}$. It should be noted that while the saturation concentration of HBr/Br_2 is reported in the literature to be very high [34], the authors appear not to account for the volume of positive electrolyte in the energy density calculation.

RFBs based on aqueous electrolyte, such as those highlighted above, are limited to a maximum V_{cell} of *ca.* 1.5 V, beyond which, electrolysis of water occurs. Without targeted modification, the solubility of POMs in non-aqueous solvent is limited. In an effort to enhance the solubility of SiV_3W_9 in non-aqueous solvent, Anderson and co-workers conducted metathesis of the potassium counter cations to tetrabutylammonium (TBA) [29]. The TBA analogue of SiV_3W_9 was soluble in acetonitrile, propylene carbonate and methanol, but the redox processes became electrochemically irreversible in propylene carbonate, and was not explored further.

Barteau and colleagues were the first to report the application of POMs as charge carrier in non-aqueous RFBs [35]. They investigated the lithium salt of the Keggin

phosphomolybdate, $\text{Li}_3[\text{PMo}_{12}\text{O}_{40}]$ (PMo_{12}), in acetonitrile with lithium trifluoromethanesulfonate (LiTf) supporting electrolyte. PMo_{12} undergoes two, one-electron quasi-reversible reductions centred at -0.21 V and -0.57 V vs. Ag/Ag^+ . For application in a symmetric system, the PMo_{12} electrolyte was first electrochemically reduced by one-electron to generate the discharged positive and negative electrolyte. Galvanostatic cycling was conducted with a one-electron redox reaction upon charge/discharge. As stated by the authors, this system does not exploit the full capabilities of POMs as multi-electron charge carriers nor the wide electrochemical stability window of non-aqueous solvents. Coulombic efficiency of 68% was achieved, which was substantially lower than that achieved for aqueous POM-based RFB. The low coulombic efficiency was attributed to crossover of the POM through the membrane, a common cause of inefficiency in non-aqueous RFBs. The saturation concentration of PMo_{12} in acetonitrile is relatively high at 0.8 M, but with only a one-electron redox reaction and V_{cell} of 0.35 V, the theoretical volumetric energy density was calculated to be 3.8 Wh L^{-1} .

While PMo_{12} can be reversibly reduced by two electrons in acetonitrile, the authors report the advantage of dimethylformamide (DMF) solvent in enhancing the electrochemical properties of the charge carrier [36]. In DMF, PMo_{12} can be reduced by an additional two electrons, enhancing the number of electrons transferred in the charge/discharge redox reaction to two and increasing V_{cell} to 0.45 V. The saturation concentration of PMo_{12} in DMF was reported to be 1.2 M, enhancing the theoretical energy density to 14.5 Wh L^{-1} . Barteau and co-workers later expanded the investigation to include an asymmetric RFB with PMo_{12} as charge carrier in the positive electrolyte and P_2W_{18} in the negative electrolyte [36]. The systems had a V_{cell} of 1.3 V and the number of electrons transferred upon charge/discharge increased to four, thereby further enhancing energy density.

The first example of significant molecular engineering of POMs to enhance solubility in non-aqueous solvent came from Matson and co-workers who investigated polyoxovanadate (POV) alkoxide clusters of the general formula $\text{V}_6\text{O}_7(\text{OR})_{12}$ (where $\text{R} = \text{CH}_3, \text{C}_2\text{H}_5$) [37]. These materials display four one-electron redox couples over a potential range of 2 V, enabling their application in a symmetric system with two-electron transfer upon charge/discharge. Upon charge the POV undergoes a two-electron reduction at the negative electrode concurrently with a two-electron oxidation at the positive electrode. The research was extended to investigate alternative organic functionalisation of the POV surface. Introduction of a tridentate tris(hydroxymethyl)methane (TRIOH) ligand, increases solubility in acetonitrile to 0.6 M and retains the charge carriers cycling stability [38]. In a separate study, the solubility of POVs was increased by replacing several surface alkoxy groups with ethers, $\text{R} = \text{C}_2\text{H}_4\text{OCH}_3, \text{C}_2\text{H}_4\text{OC}_2\text{H}_5$ [39]. Clusters with a mixture of alkoxide and ether groups showed an impressive solubility of 1.2 M in 0.1 M $[\text{TBA}][\text{PF}_6]$ in acetonitrile. While the increased solubility in organic solvent and multi-electron redox chemistry is promising for enhanced energy density, preliminary testing of the alkoxide-ether functionalised POVs in a laboratory-scale RFB showed steady capacity fade. Cyclic voltammetry of electrolytes following 30 cycles in a RFB indicated partial degradation of the POV clusters. For further reading on POV-based charge carriers for RFBs, we direct readers to a recent review article [40].

The concept of organofunctionalisation of POMs to enhance solubility in non-aqueous solvent was expanded in a recent publication, to include organic-inorganic hybrid POMs [41]. A phosphotungstate Keggin was hybridised with phenyl siloxane

moieties to produce $\text{TBA}_3[\text{PW}_{11}\text{O}_{39}(\text{SiC}_6\text{H}_5)_2\text{O}]$ ($\text{PW}_{11}\text{SiPh}$). Hybridisation enhanced solubility in acetonitrile by two orders of magnitude (0.6 M) compared to the parent POM (<1 mM). Similarly to POVs, $\text{PW}_{11}\text{SiPh}$ displays four one-electron redox couples over a potential range of 2 V. Prior to galvanostatic cycling the electrolyte was reduced by bulk electrolysis to attain the discharged positive and negative electrolyte for application in a symmetric system. Upon charge, $\text{PW}_{11}\text{SiPh}$ undergoes a two-electron reduction at the negative electrode concurrently with a two-electron oxidation at the positive electrode. The laboratory-scale RFB achieved high coulombic efficiency of >98% but capacity fade was observed. Similarly to Stimming and colleagues, the capacity fade was attributed to reoxidation of the reduced POM by trace oxygen in the electrolyte. Capacity fade was shown to be recoverable by bulk reduction of the electrolytes to the desired oxidation state. Organic-inorganic hybridisation is applicable to a broad range of POM geometries and elemental compositions, unlocking the possibility for the development of multi-electron charge carriers across a wide potential range (**Figure 7**).

Yan and colleagues explored the use of a sulphur-templated Wells-Dawson POM, $\text{TBA}_4[\text{S}_2\text{W}_{18}\text{O}_{62}]$ (S_2W_{18}), as charge carrier in both symmetric and asymmetric non-aqueous RFBs [42]. In the asymmetric system benzophenone was chosen as the negative electrolyte. Benzophenone undergoes a reversible one-electron reduction with redox potential of -1.75 V vs. $\text{Ag}^+|\text{Ag}$ (see **Figure 3**), while S_2W_{18} can be reversibly reduced by one, one, then two electrons with redox potentials of 0.23, -0.15 and -0.49 V vs. $\text{Ag}^+|\text{Ag}$. In the asymmetric RFB, four equivalents of benzophenone were used to balance the four-electron redox process of S_2W_{18} . Although not stated by the authors, reduction of S_2W_{18} to generate discharged positive electrolyte (or reduction of benzophenone to generate charged negative electrolyte) would have been necessary prior to galvanostatic cycling. The flow cell cycled successfully with V_{cell} of 1.54 V. Based on the saturation concentration of S_2W_{18} in acetonitrile of 0.11 M, the theoretical energy density was calculated to be 9.4 Wh L^{-1} .

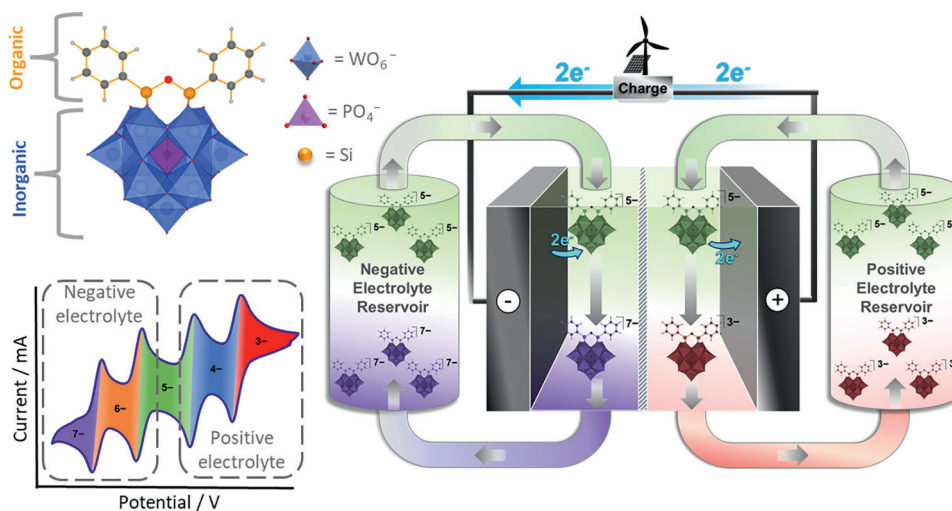


Figure 7. Structure, cyclic voltammogram and RFB schematic of $\text{PW}_{11}\text{SiPh}$, an organic-inorganic hybrid POM charge carrier. Figure was adapted with permission from [41] Copyright © 2021, American Chemical Society.

5. Conclusions

The use of multi-electron charge carriers is an effective approach to enhance the energy density of next-generation RFBs. Polyoxometalates stand out as a particularly promising class of materials due to their remarkably rich and reversible electrochemical properties. This is elegantly demonstrated by the 18-electron reversible reduction of P_2W_{18} , yielding an asymmetric RFB with practical energy density of 225 Wh L^{-1} . Organofunctionalisation of polyoxometalates is a valuable strategy to enhance solubility in non-aqueous solvent and for the tuning of redox properties and chemical stability. Other multi-electron charge carriers, such as metal-coordination complexes and bifunctional molecules, are realised through targeted molecular design and synthesis. Their rich electrochemical properties allow for their application in symmetric RFBs, thereby reducing the risk of capacity fade by membrane crossover. The bifunctional charge carriers also benefit from higher solubility than the isolated redox-active molecules.

Increasing the number of electrons transferred per molecule is a valuable strategy to enhance the energy density of RFBs. However, this parameter should not be targeted in isolation and should be considered alongside solubility, redox potential targeting, stability, cost and sustainability. In addition, the development of charge carriers for next-generation RFBs requires consideration of the flow cell assembly used for testing. Charge carrier performance depends on components such as membrane and tubing, and on the testing conditions such as flow rate, current density, and voltage thresholds. The lack of standardisation in testing conditions make it challenging to compare the performance of charge carriers.

The research reviewed here focuses on the development of novel charge carriers to enhance RFB performance. Most testing is conducted at low concentrations and in laboratory-scale RFBs. As the research matures, testing at scales more representative of the commercial product and detailed techno-economic analysis of the charge carrier-containing electrolyte will be required. Assessment of the costs of charge carriers, sustainability, safety, and practicality of synthesis will become increasingly important in the development of commercially viable next-generation RFBs.

Acknowledgements

The authors gratefully acknowledge the Engineering and Physical Sciences Research Council (EPSRC) for funding through the Centre for Doctoral Training in Sustainable Chemistry (EP/L015633/1). We also thank the University of Nottingham Propulsion Futures Beacon of Excellence for support.

Conflict of interest

There are no conflicts to declare.

Appendices and nomenclature

bpy	bipyridine
DMF	dimethylformamide
LIB	lithium-ion battery


POM	polyoxometalate
POV	polyoxovanadate
RFB	redox flow battery
TBA	tetrabutylammonium

Author details

Catherine L. Peake, Graham N. Newton* and Darren A. Walsh*
Nottingham Applied Materials and Interfaces (NAMI), The GSK Carbon Neutral
Laboratories for Sustainable Chemistry, University of Nottingham, UK

*Address all correspondence to: graham.newton@nottingham.ac.uk
and darren.walsh@nottingham.ac.uk

IntechOpen

© 2022 The Author(s). Licensee IntechOpen. This chapter is distributed under the terms of the Creative Commons Attribution License (<http://creativecommons.org/licenses/by/3.0>), which permits unrestricted use, distribution, and reproduction in any medium, provided the original work is properly cited. 

References

- [1] Gür TM. Review of electrical energy storage technologies, materials and systems: Challenges and prospects for large-scale grid storage. *Energy & Environmental Science*. 2018;**11**(10):2696-2767
- [2] Cameron JM, Holc C, Kibler AJ, Peake CL, Walsh DA, Newton GN, et al. Molecular redox species for next-generation batteries. *Chemical Society Reviews*. 2021;**50**:5863-5883
- [3] Sánchez-Díez E, Ventosa E, Guarnieri M, Trovò A, Flox C, Marcilla R, et al. Redox flow batteries: Status and perspective towards sustainable stationary energy storage. *Journal of Power Sources*. 2021;**481**:228804
- [4] Leung P, Li X, Ponce De León C, Berlouis L, Low CTJ, Walsh FC. Progress in redox flow batteries, remaining challenges and their applications in energy storage. *RSC Advances*. 2012;**2**(27):10125-10156
- [5] Thaller L. Redox flow cell energy storage systems. In: *Terrestrial Energy Systems Conference Proceeding*; Orlando, Florida, US. Cleveland, Ohio, USA: National Aeronautics and Space Administration; 1979
- [6] Roe S, Menictas C, Skyllas-Kazacos M. A high energy density vanadium redox flow battery with 3 M vanadium electrolyte. *Journal of the Electrochemical Society*. 2016;**163**(1):A5023-A5028
- [7] Zhao P, Zhang H, Zhou H, Chen J, Gao S, Yi B. Characteristics and performance of 10 kW class all-vanadium redox-flow battery stack. *Journal of Power Sources*. 2006;**162**(2):1416-1420
- [8] Vanitec. Vanadium Redox Flow Battery Companies [Internet]. 2021. Available from: <http://www.vanitec.org/vanadium-redox-flow-battery-vrfb-companies>
- [9] Dmello R, Milshtein JD, Brushett FR, Smith KC. Cost-driven materials selection criteria for redox flow battery electrolytes. *Journal of Power Sources*. 2016;**330**:261-272
- [10] GRIDS: Grid-Scale Rampable Intermittent Dispatchable Storage. USA: US Department of Energy; 2010. Available from: www.osti.gov/biblio/1046668
- [11] Trahey L, Brushett FR, Balsara NP, Ceder G, Cheng L, Chiang YM, et al. Energy storage emerging: A perspective from the Joint Center for Energy Storage Research. *Proceedings of the National Academy of Sciences of the United States of America*. 2020;**117**(23):12550-12557
- [12] Lourenssen K, Williams J, Ahmadpour F, Clemmer R, Tasnim S. Vanadium redox flow batteries: A comprehensive review. *J Energy Storage*. 2019;**25**:100844
- [13] Gong K, Fang Q, Gu S, Fong S, Li Y, Yan Y. Nonaqueous redox-flow batteries: Organic solvents, supporting electrolytes, and redox pairs. *Energy Environmental Science*. 2015;**8**(8):3515-3530
- [14] Yuan J, Pan ZZ, Jin Y, Qiu Q, Zhang C, Zhao Y, et al. Membranes in non-aqueous redox flow battery: A review. *Journal of Power Sources*. 2021;**500**:229983

- [15] Prifti H, Parasuraman A, Winardi S, Lim TM, Skyllas-Kazacos M. Membranes for redox flow battery applications. *Membranes (Basel)*. 2012;**2**:275-306
- [16] Wei X, Pan W, Duan W, Hollas A, Yang Z, Li B, et al. Materials and systems for organic redox flow batteries: Status and challenges. *ACS Energy Letters*. 2017;**2**:2187-2204
- [17] Winsberg J, Hagemann T, Janoschka T, Hager MD, Schubert US. Redox-flow batteries: From metals to oRedox-active materials. *Angewandte Chemie, International Edition*. 2017;**56**(3):686-711
- [18] Li M, Rhodes Z, Cabrera-Pardo JR, Minter SD. Recent advancements in rational design of non-aqueous organic redox flow batteries. *Sustainable Energy & Fuels*. 2020;**4**(9):4370-4389
- [19] Ding Y, Zhang C, Zhang L, Zhou Y, Yu G. Molecular engineering of organic electroactive materials for redox flow batteries. *Chemical Society Reviews*. 2018;**47**(1):69-103
- [20] Sivaraman N, Dhamodaran R, Kaliappan I, Srinivasan TG, Rao PRV, Mathews CK. Solubility of C60 in organic solvents. *The Journal of Organic Chemistry*. 1992;**57**(22):6077-6079
- [21] Friedl J, Lebedeva MA, Porfyrakis K, Stimming U, Chamberlain TW. All fullerene-based cells for non-aqueous redox flow batteries. *Journal of the American Chemical Society*. 2018;**140**:401-405
- [22] Ruoff RS, Tse DS, Malhotra R, Lorents DC. Solubility of C60 in a variety of solvents. *The Journal of Physical Chemistry*. 1993;**97**(13):3379-3383
- [23] Winsberg J, Stolze C, Muench S, Liedl F, Hager MD, Schubert US. TEMPO/phenazine combi-molecule: A redox-active material for symmetric aqueous redox-flow batteries. *ACS Energy Letters*. 2016;**1**(5):976-980
- [24] Hogue RW, Toghiani KE. Metal coordination complexes in nonaqueous redox flow batteries. *Current Opinion in Electrochemistry*. 2019;**18**:37-45
- [25] Matsuda Y, Tanaka K, Okada M, Takasu Y, Morita M, Matsumura-Inoue T. A rechargeable redox battery utilizing ruthenium complexes with non-aqueous organic electrolyte. *Journal of Applied Electrochemistry*. 1988;**18**(6):909-914
- [26] Palmer TC, Beamer A, Pitt A, Popov IA, Cammack CX, Pratt HD, et al. A comparative review of metal-based charge carriers in nonaqueous flow batteries. *ChemSusChem*. 2021;**14**(5):1214-1228
- [27] Cabrera PJ, Yang X, Suttill JA, Hawthorne KL, Brooner REM, Sanford MS, et al. Complexes containing redox noninnocent ligands for symmetric, multielectron transfer nonaqueous redox flow batteries. *Journal of Physical Chemistry C*. 2015;**119**(28):15882-15889
- [28] Li Q, Zhang L, Dai J, Tang H, Li Q, Xue H, et al. Polyoxometalate-based materials for advanced electrochemical energy conversion and storage. *Chemical Engineering Journal*. 2018;**351**:441-461
- [29] Pratt HD, Hudak NS, Fang X, Anderson TM. A polyoxometalate flow battery. *Journal of Power Sources*. 2013;**236**:259-264
- [30] Liu Y, Lu S, Wang H, Yang C, Su X, Xiang Y. An aqueous redox flow battery with a tungsten-cobalt heteropolyacid as the electrolyte for both the anode and cathode. *Advanced Energy Materials*. 2017;**7**(8):1601224

- [31] Friedl J, Holland-Cunz MV, Cording F, Pfanschilling FL, Wills C, McFarlane W, et al. Asymmetric polyoxometalate electrolytes for advanced redox flow batteries. *Energy & Environmental Science*. 2018;**11**(10):3010-3018
- [32] Friedl J, Pfanschilling FL, Holland-Cunz MV, Fleck R, Schrickler B, Wolfschmidt H, et al. A polyoxometalate redox flow battery: Functionality and upscale. *Clean Energy*. 2019;**3**(4):278-287
- [33] Chen JJ, Symes MD, Cronin L. Highly reduced and protonated aqueous solutions of [P2W18O62]6- for on-demand hydrogen generation and energy storage. *Nature Chemistry*. 2018;**10**(10):1042-1047
- [34] Küttinger M, Wlodarczyk JK, Daubner D, Fischer P, Tübke J. High energy density electrolytes for H2/Br2 redox flow batteries, their polybromide composition and influence on battery cycling limits. *RSC Advances*. 2021;**11**(9):5218-5229
- [35] Chen JJJ, Barteau MA. Molybdenum polyoxometalates as active species for energy storage in non-aqueous media. *Journal of Energy Storage*. 2017;**13**:255-261
- [36] Cao Y, Chen JJJ, Barteau MA. Systematic approaches to improving the performance of polyoxometalates in non-aqueous redox flow batteries. *Journal of Energy Chemistry*. 2020;**50**:115-124
- [37] Vangelder LE, Kosswatta arachchi AM, Forrestel PL, Cook TR, Matson EM. Polyoxovanadate-alkoxide clusters as multi-electron charge carriers for symmetric non-aqueous redox flow batteries. *Chemical Science*. 2018;**9**(6):1692-1699
- [38] VanGelder LE, Petel BE, Nachtigall O, Martinez G, Brennessel WW, Matson EM. Organic functionalization of polyoxovanadate-alkoxide clusters: Improving the solubility of multimetallic charge carriers for nonaqueous redox flow batteries. *ChemSusChem*. 2018;**11**(23):4139-4149
- [39] Vangelder LE, Pratt HD, Anderson TM, Matson EM. Surface functionalization of polyoxovanadium clusters: Generation of highly soluble charge carriers for nonaqueous energy storage. *Chemical Communications*. 2019;**55**(81):12247-12250
- [40] VanGelder LE, Cook TR, Matson EM. Progress in the design of polyoxovanadate-alkoxides as charge carriers for nonaqueous redox flow batteries. *Comments on Inorganic Chemistry*. 2019;**39**(2):51-89
- [41] Peake CL, Kibler AJ, Newton GN, Walsh DA. Organic-inorganic hybrid polyoxotungstates as configurable charge carriers for high energy redox flow batteries. *ACS Applied Energy Mater*. 2021;**4**(9):8765-8773
- [42] Chen ZF, Yang YL, Zhang C, Liu SQ, Yan J. Manufacture of non-aqueous redox flow batteries using sulfate-templated Dawson-type polyoxometalate with improved performances. *Journal of Energy Storage*. 2021;**35**:102281